Electronic Supplementary Information for:

Redox Properties of [Cp*Rh] Complexes Supported by Mono-substituted 2,2′-Bipyridyl Ligands

*Jonah P. Stiel,[a,‡] Wade C. Henke,[a,§] William N. G. Moore,[a,‡] Nathaniel M. Barker,[b,#] Allen G. Oliver,[b] Victor W. Day,[a] and James D. Blakemore[a,]**

[a] Department of Chemistry, University of Kansas,
1567 Irving Hill Road, Lawrence, Kansas 66045, United States.

[b] Department of Chemistry & Biochemistry, University of Notre Dame,
149 Stepan Chemistry Hall, Notre Dame, Indiana 46545, United States.

‡ Current address: Department of Chemistry, University of California at Irvine,
Irvine, California 92617, United States.

§ Current address: Procter & Gamble, North Chicago Plant,
3500 16th St, North Chicago, Illinois 60064, United States.

Current address: Integrated Molecular Structure Education and Research Center (IMSERC),
Northwestern University, Evanston, Illinois 60208, United States.

* To whom correspondence should be addressed. E-mail: blakemore@ku.edu (J.D.B.).

Nuclear Magnetic Resonance (NMR)

Mass Spectrometry

Electron Absorption Spectroscopy

Electrochemistry

Spectrochemical Titrations

Crystallographic Information

Nuclear Magnetic Resonance (NMR) Spectroscopy

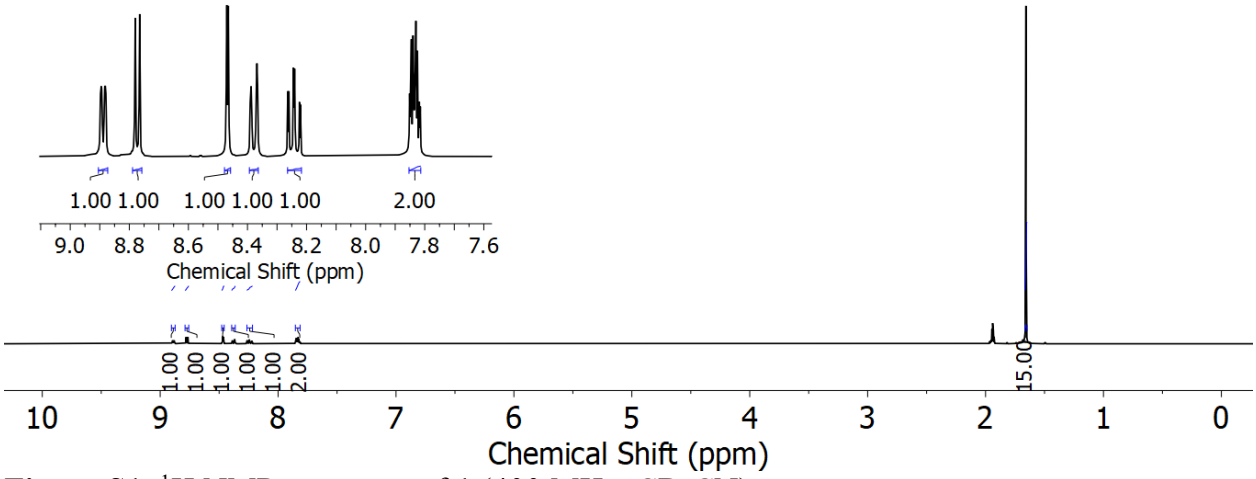

Figure S1. ^{1}H NMR spectrum of **1** (400 MHz, CD_3CN).

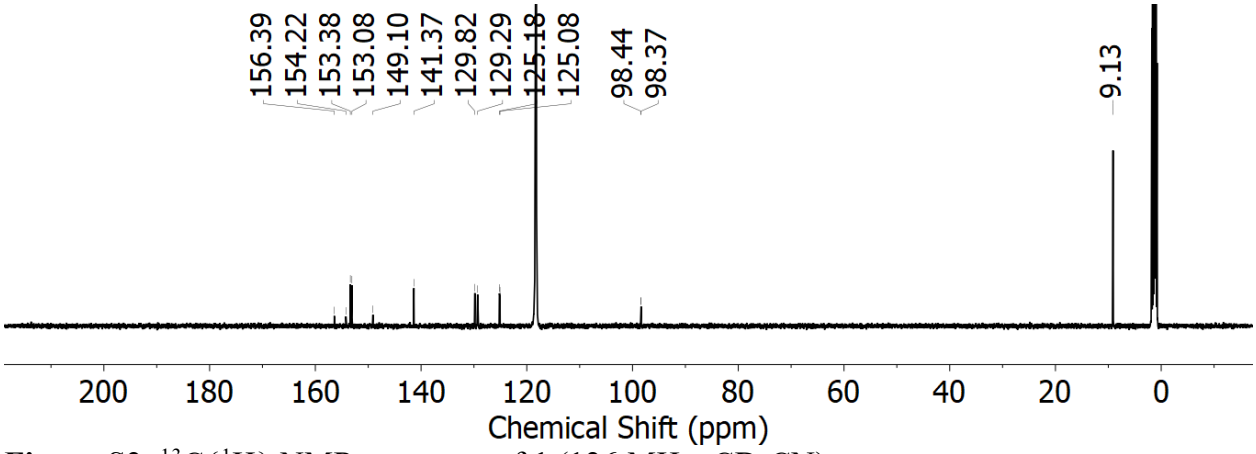

Figure S2. $^{13}C\{^{1}H\}$ NMR spectrum of **1** (126 MHz, CD_3CN).

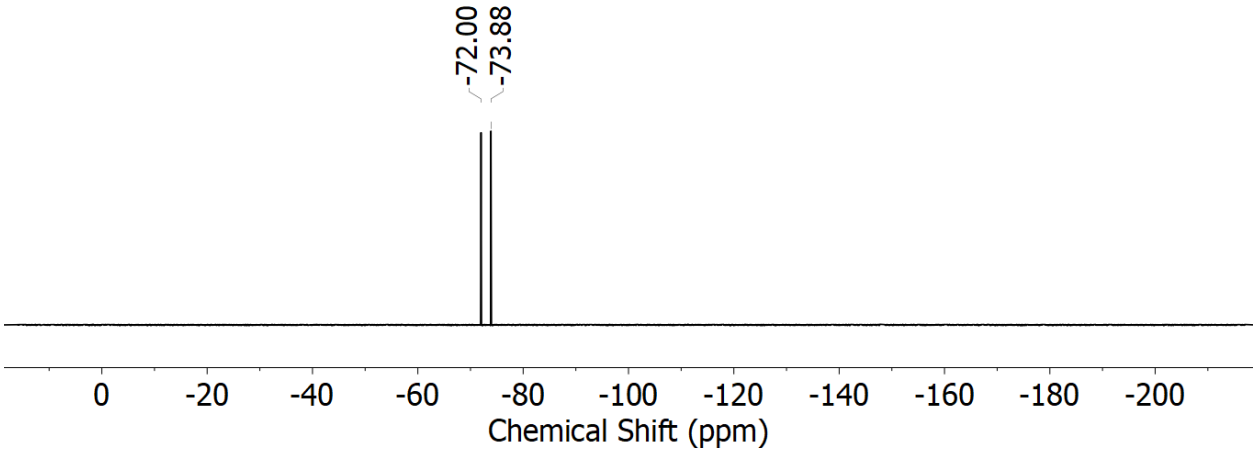

Figure S3. ^{19}F NMR spectrum of **1** (376 MHz, CD_3CN).

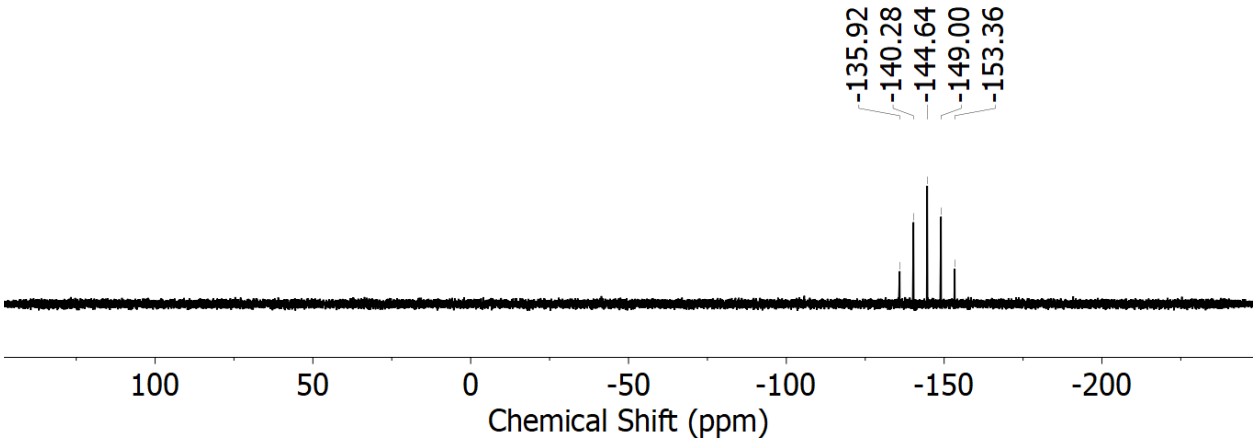

Figure S4. ^{31}P NMR spectrum of **1** (162 MHz, CD_3CN).

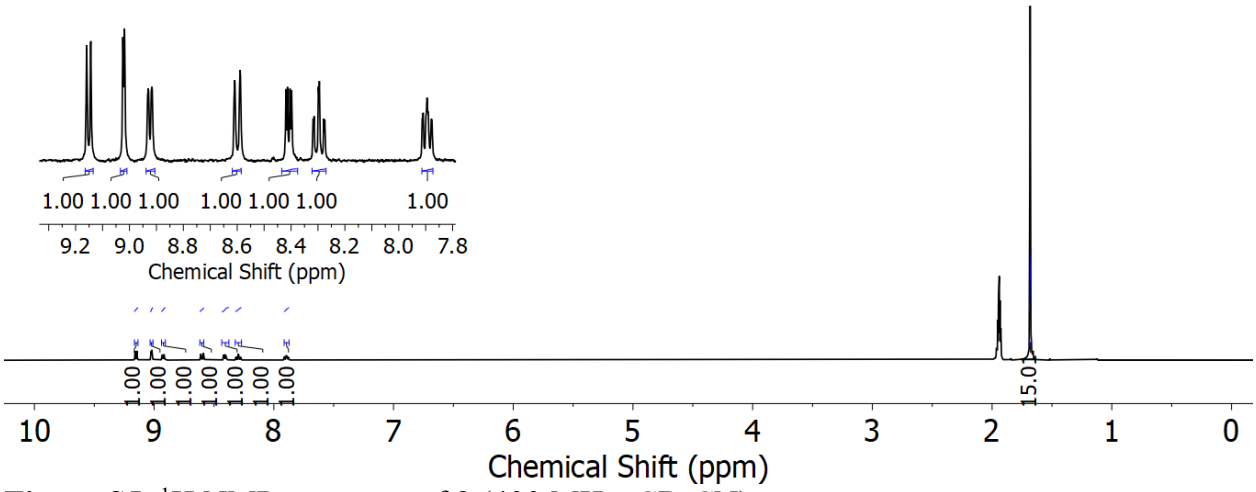

Figure S5. ^{1}H NMR spectrum of **2** (400 MHz, CD_3CN).

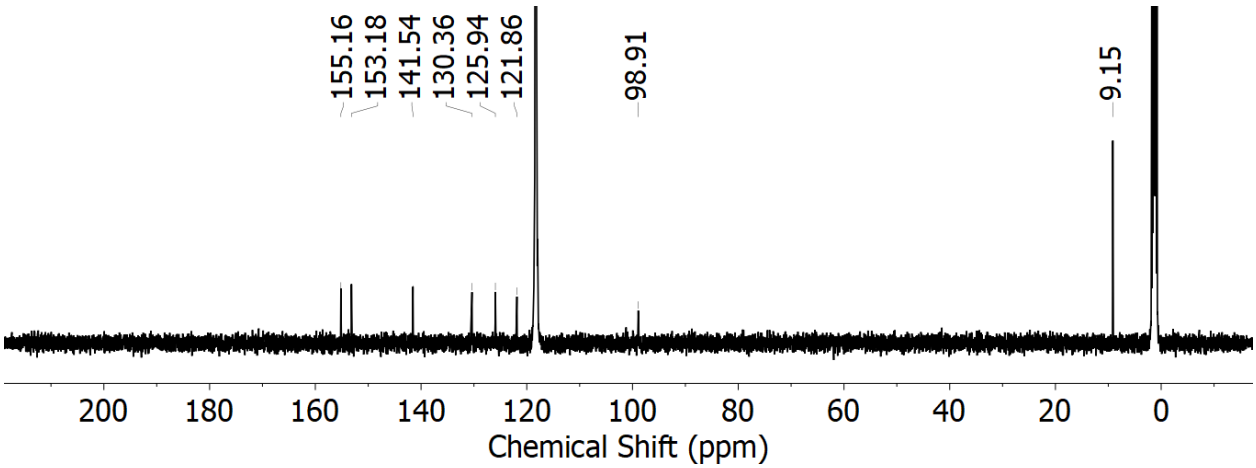

Figure S6. $^{13}C\{^{1}H\}$ NMR spectrum of **2** (126 MHz, CD_3CN).

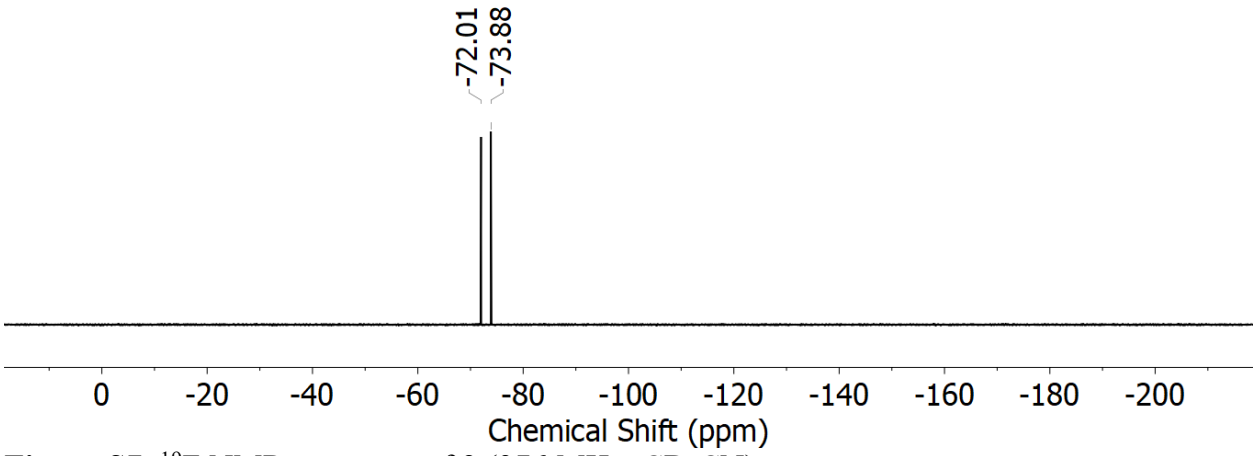

Figure S7. ^{19}F NMR spectrum of **2** (376 MHz, CD_3CN).

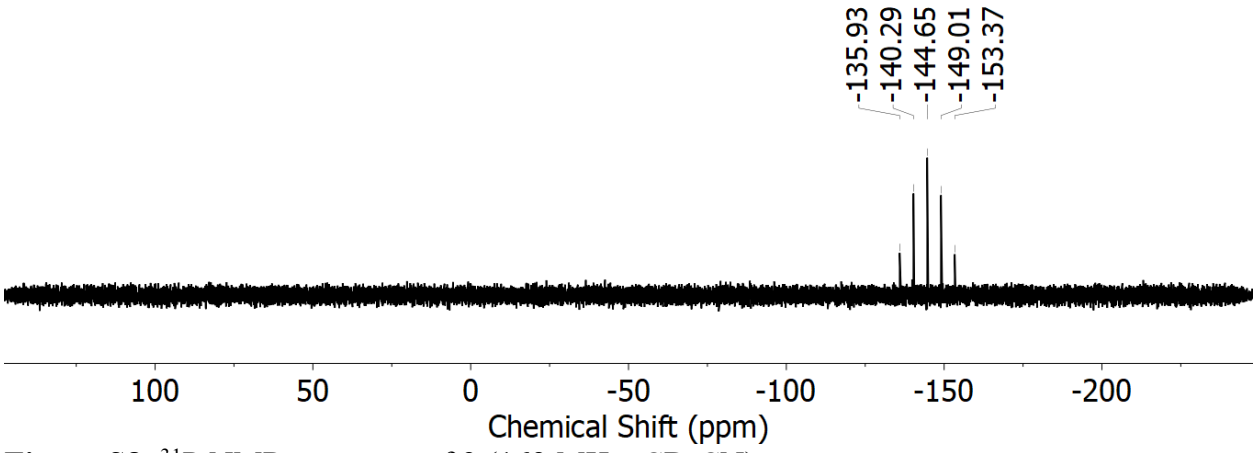

Figure S8. ^{31}P NMR spectrum of **2** (162 MHz, CD_3CN).

Mass Spectrometry

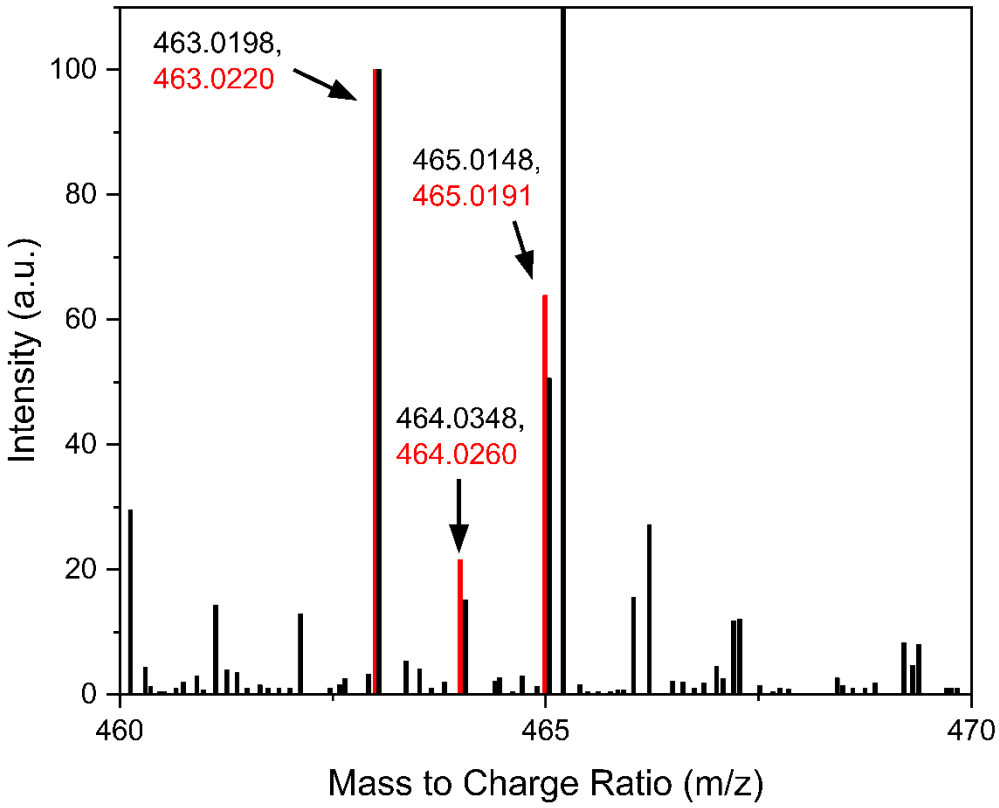

Figure S9. ESI-mass spectral data collected with **1**. The predicted parent peak represents $[Cp^*Rh(mcbpy)Cl]^+$ (**1** – PF_6^-). The experimental data is shown in **black** and the predicted data is shown in **red**. The intensity of the signal near 463 m/z was set to the intensity value of 100 a.u.

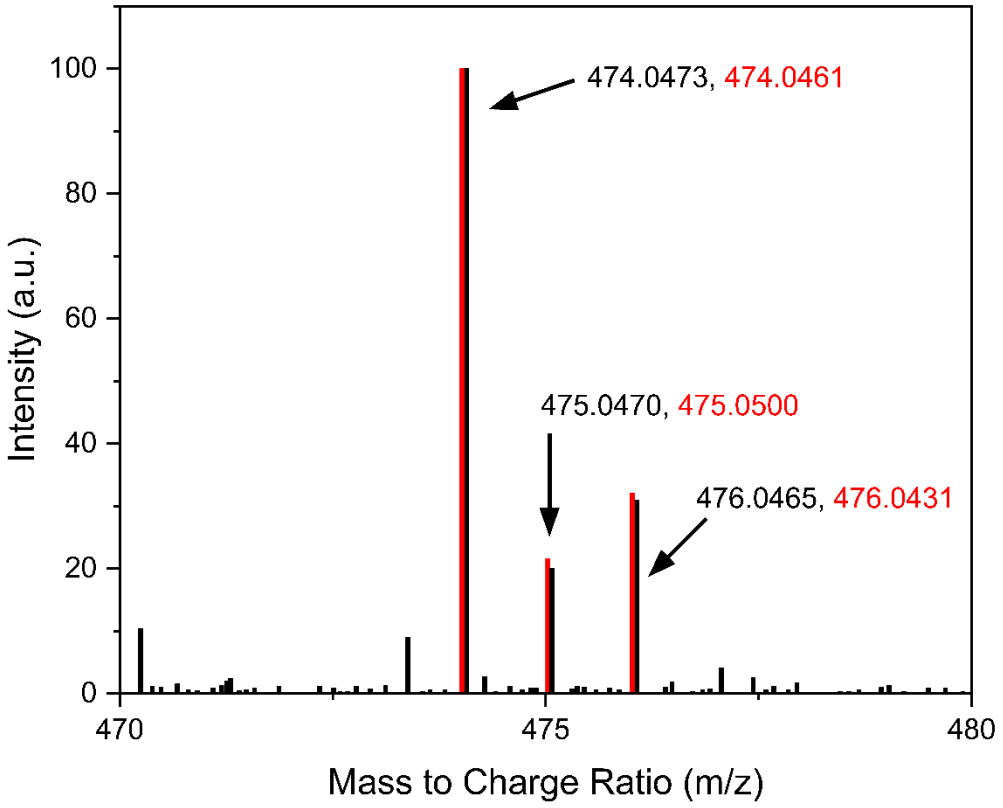

Figure S10. ESI-mass spectrum of **2**. The predicted parent peak represents $[Cp^*Rh(mnbpy)Cl]^+$ (**2** – PF_6^-). The experimental data is shown in **black** and the predicted data is shown in **red**.

Electronic Absorption Spectroscopy

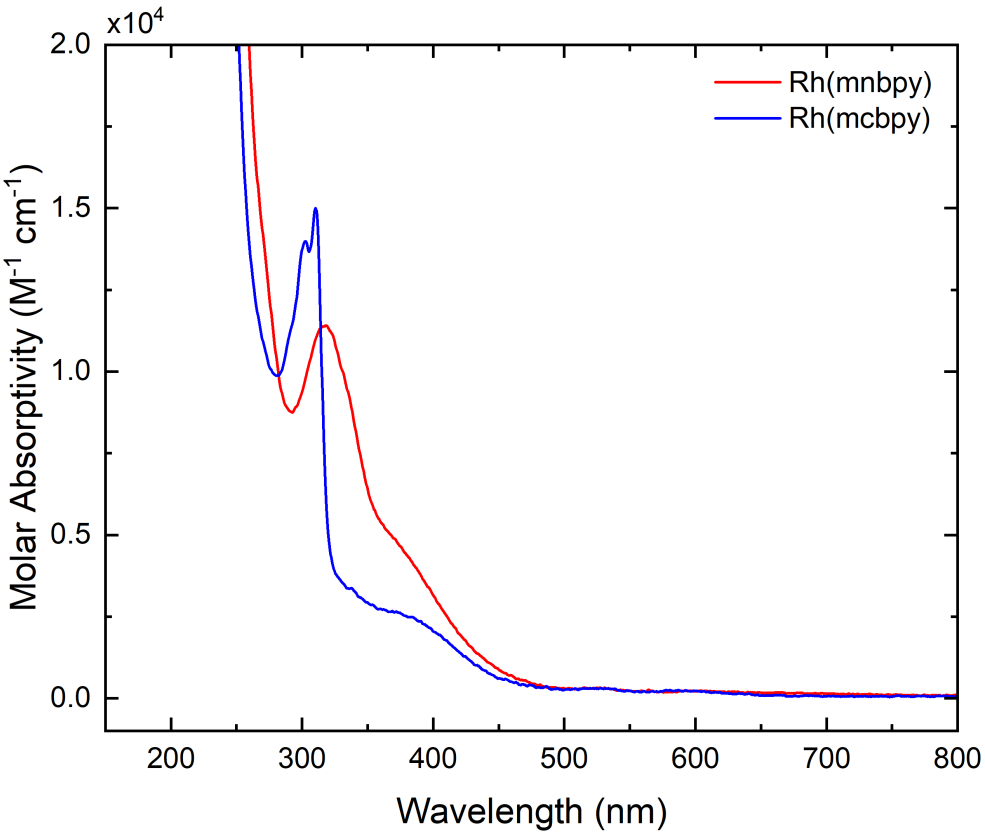

Figure S11. Electronic absorption spectrum of **1** and **2** at concentrations of 61.56 μM and 62.61 μM, respectively.

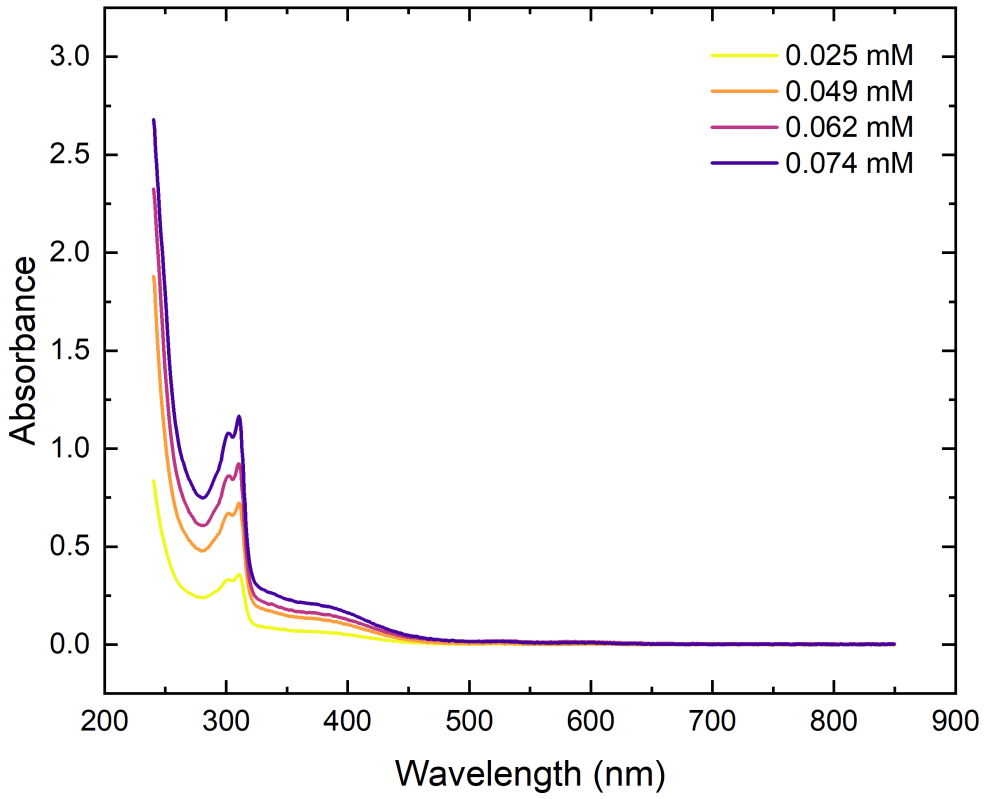

Figure S12. Electronic absorption spectra of **1** at multiple concentrations.

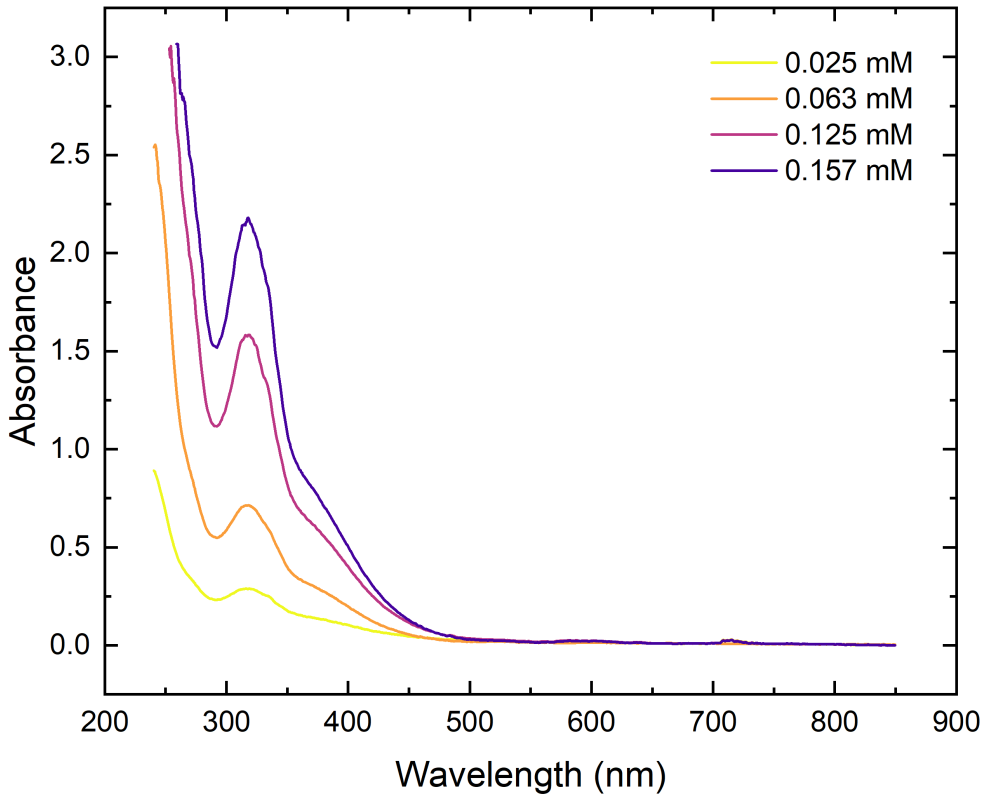

Figure S13. Electronic absorption spectra of **2** at multiple concentrations.

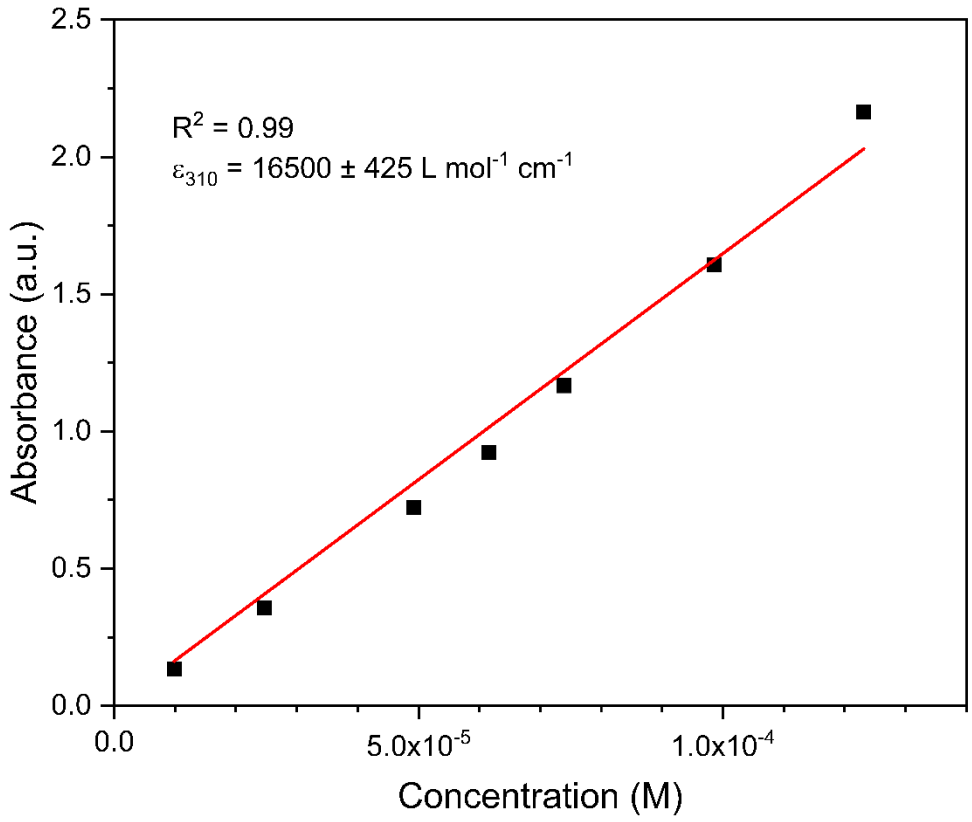

Figure S14. Molar absorptivity of **1** at multiple concentrations.

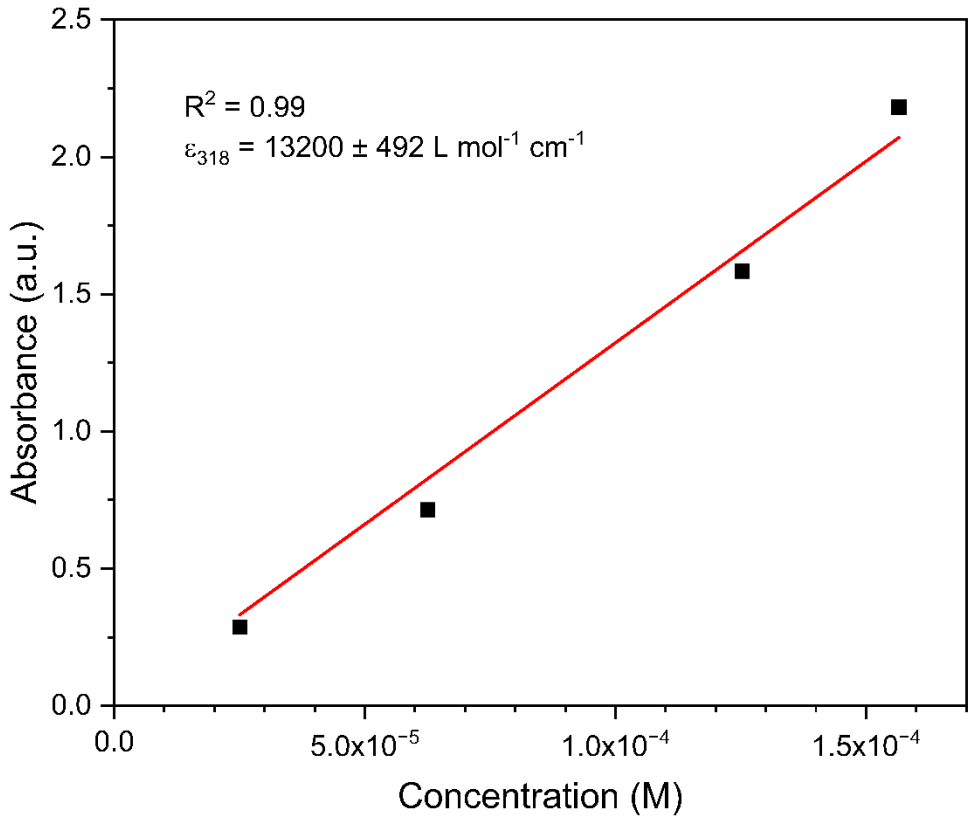

Figure S15. Molar absorptivity of **2** at multiple concentrations.

Electrochemistry

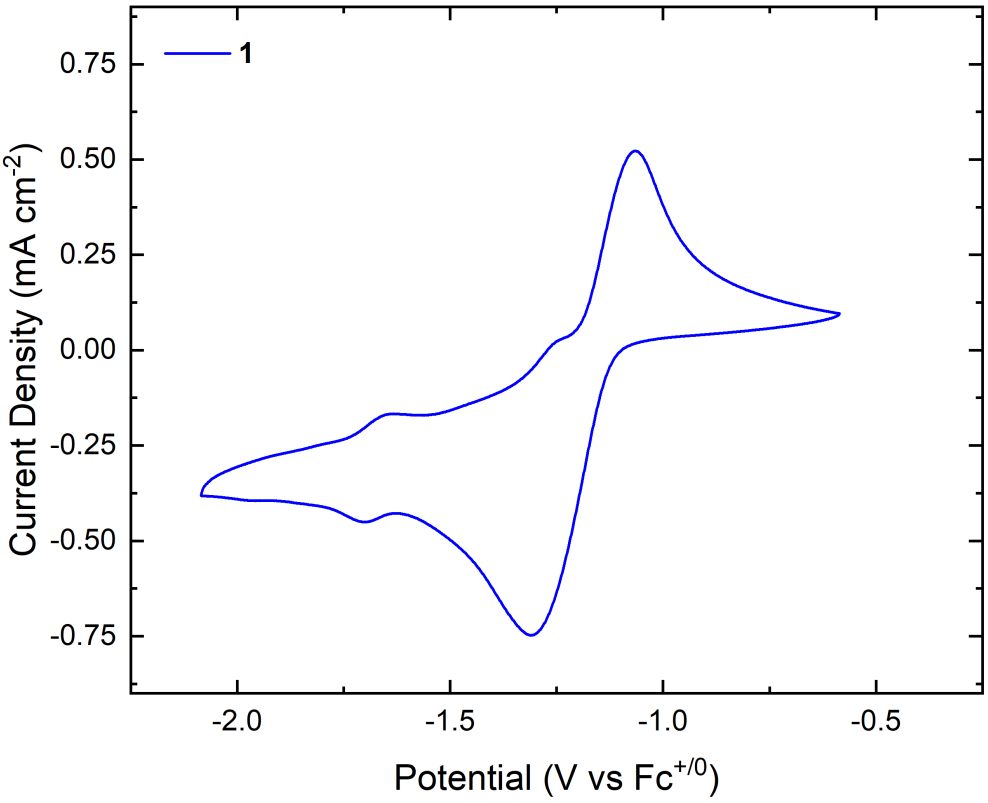

Figure S16. Cyclic voltammetry of **1** (MeCN, 0.1 M [$^{n}Bu_4N$][PF_6], 100 mV/s)

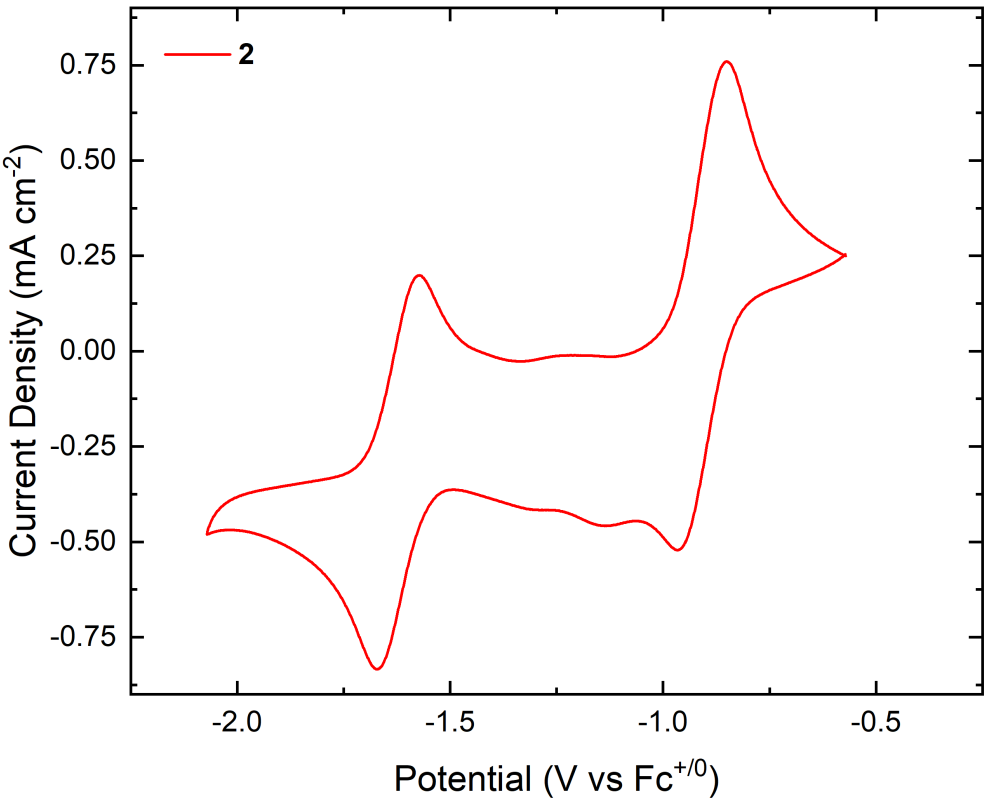

Figure S17. Cyclic voltammetry of **2** (MeCN, 0.1 M [^{n}Bu$_4$N][PF$_6$], 100 mV/s)

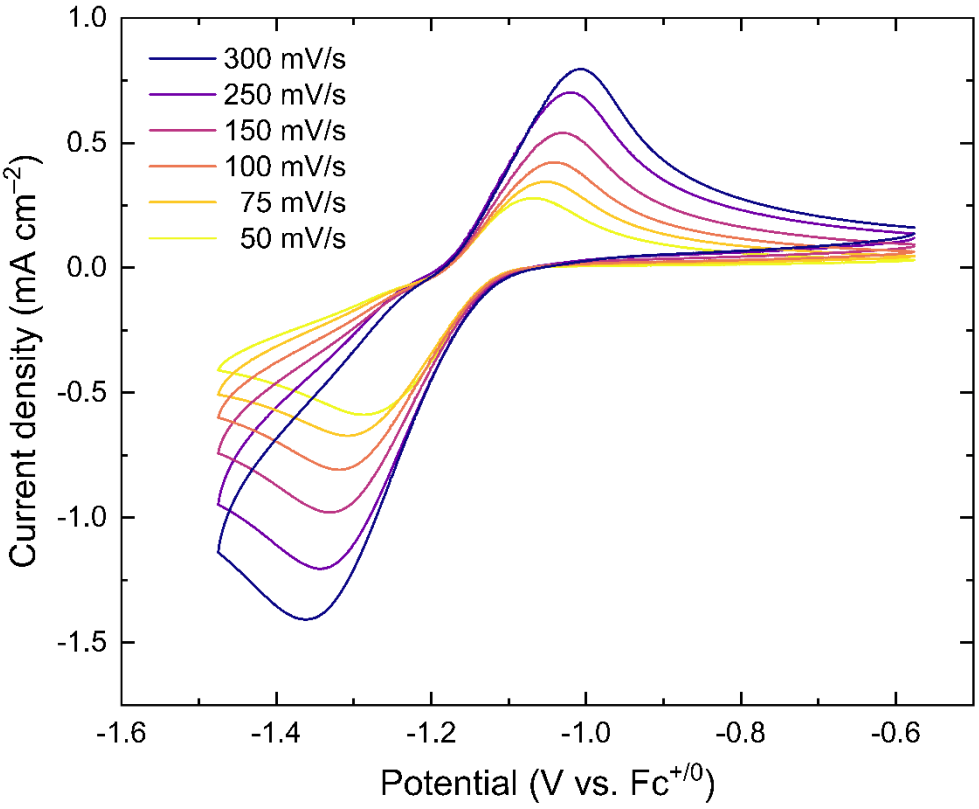

Figure S18. Cyclic voltammetry of **1** performed at multiple scan rates.

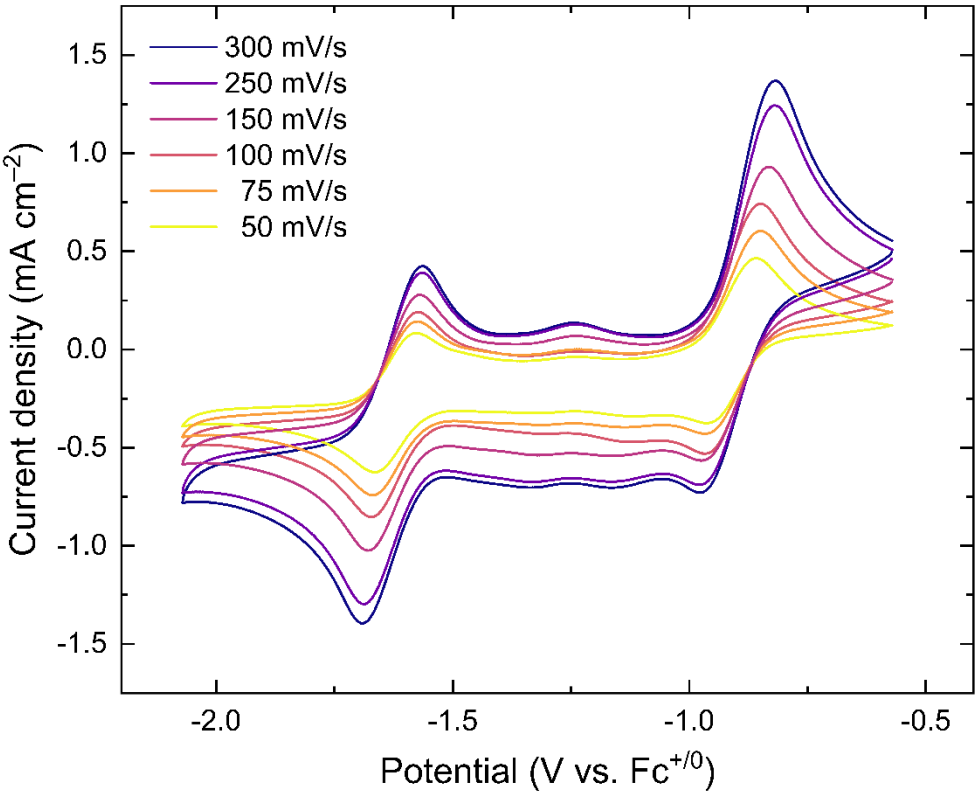

Figure S19. Cyclic voltammetry of **2** performed at multiple scan rates.

Spectrochemical Titrations

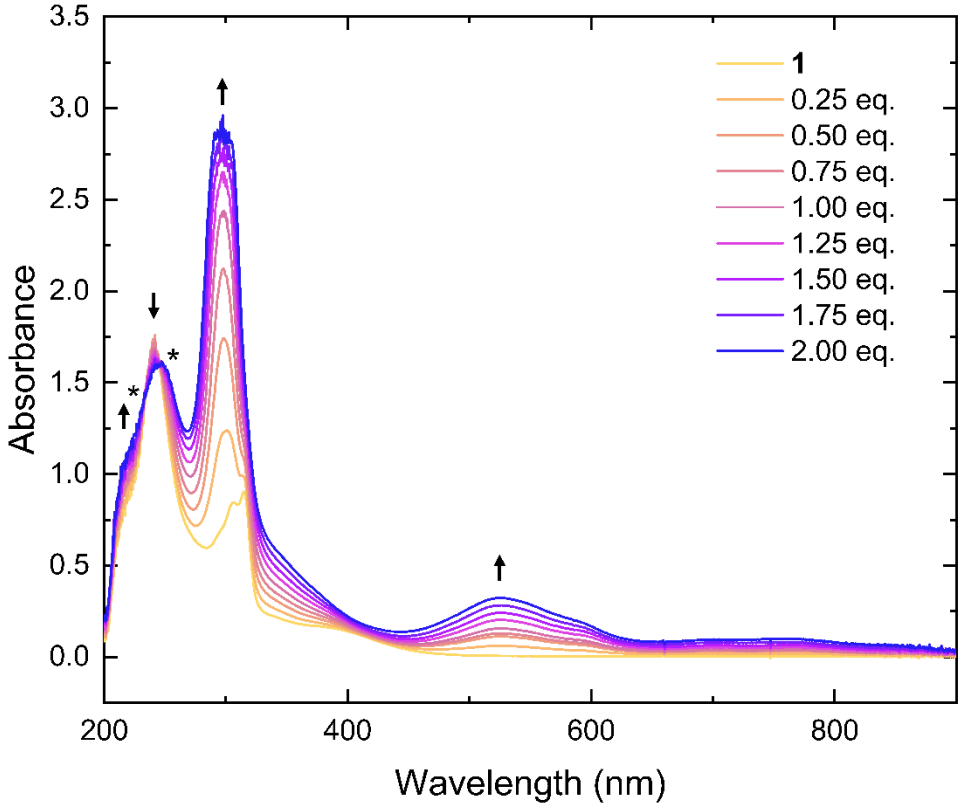

Figure S20. Spectrochemical titration of **1** with up to two equivalents of Cp^*_2Co. Isosbestic points, marked with asterisks (*), are present at 230 nm and 247 nm.

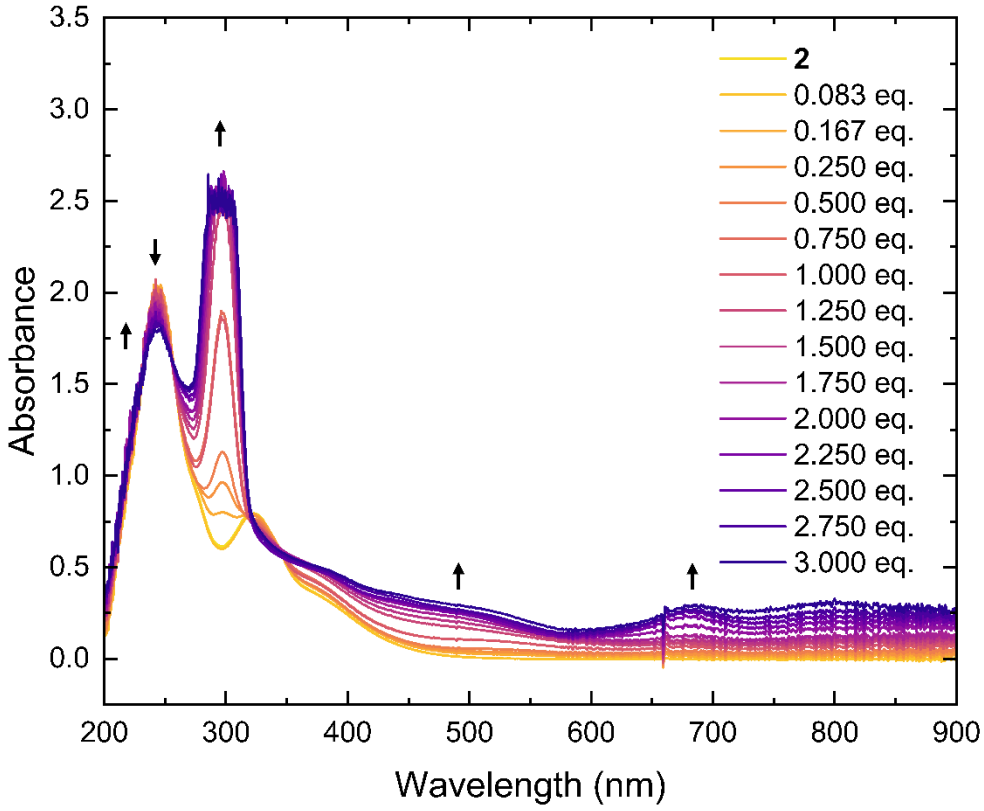

Figure S21. Spectrochemical titration of **2** with up to three equivalents of Cp^*_2Co.

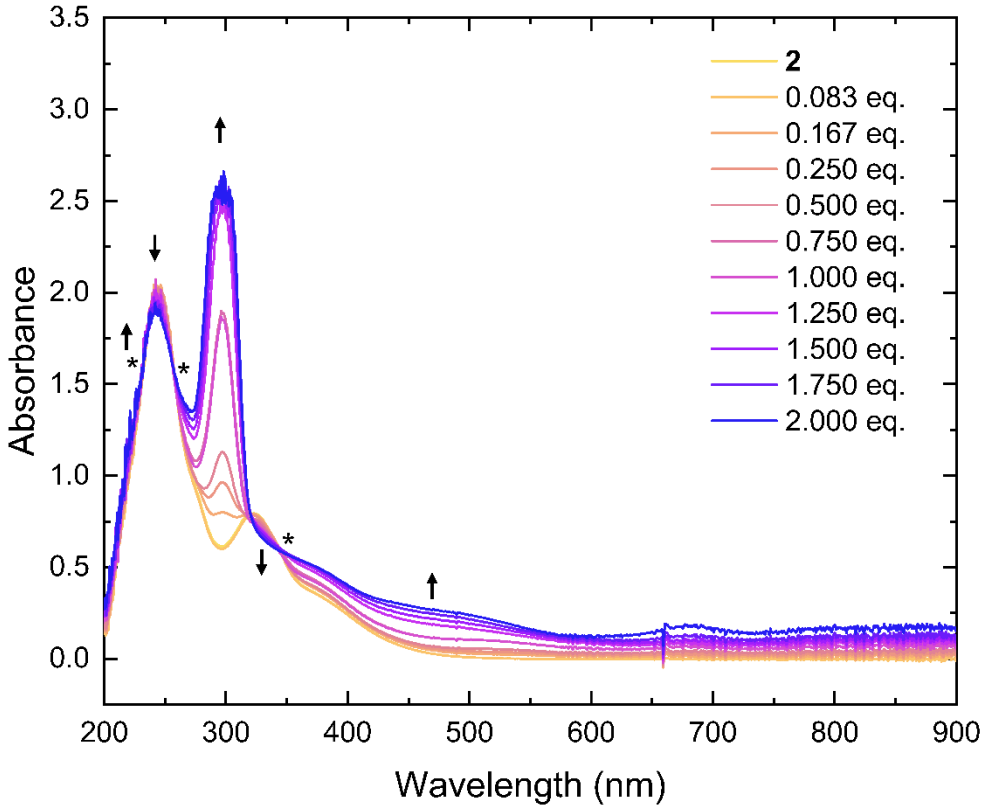

Figure S22. Spectrochemical titration of **2** with up to two equivalents of Cp^*_2Co. Isosbestic points, marked with asterisks (*), are present at 232 nm, 256 nm, and 344 nm.

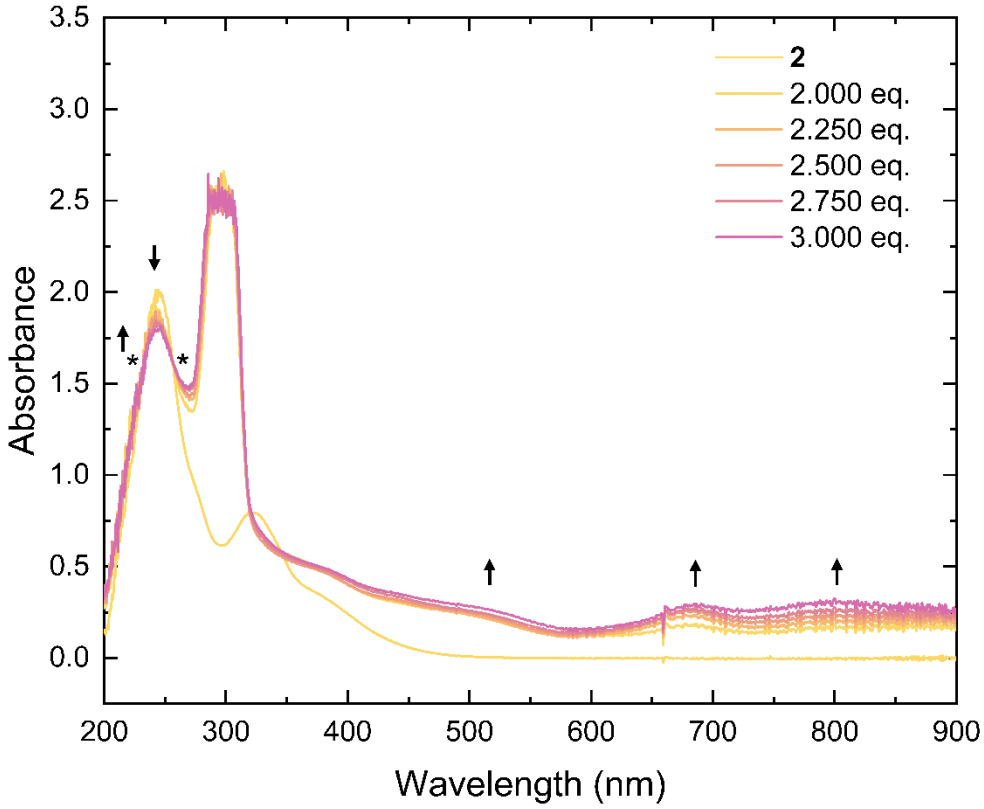

Figure S23. Spectrochemical titration of **2** with two to three equivalents of Cp^*_2Co. Isosbestic points, marked with asterisks (*), are present at 235 nm and 253 nm.

Crystallographic Information

Special Refinement Details for **1** (q01i)

The initial centrosymmetric Pbca (No. 61) structure solution for **1** exhibited Cl2/Cl2′ disorder (Figure S25) with regard to the position of the single chloride substituent on the bipyridyl ligand, a situation somewhat reminscent of the nitro compound **2** (*vide infra*). Enantiomers are formed when a single Cl binds to the two different, relevant carbon atoms at the 4 and 4′ positions on the pyridyl rings (C13 and C18). The disorder in **1** was modeled by refining the normalized relative occupancies of Cl2 and Cl2′, giving a ratio of 85/15. The occupancies of the corresponding alternate H atoms (H13′ and H18, respectively) were set at one minus the occupancy of the chlorine at those positions. The 85/15 occupancy ratio seemed to preclude the possibility that the wrong lattice constants or space group had been assigned. This structure was therefore solved and completely refined to an acceptable final R_1 value of 0.0478 in the centrosymmetric space group Pbca. This space group choice would be consistent with compound **1** being chiral with both enantiomers present in solution prior to crystallization.

Like the apparently disordered centrosymmetric structure of nitrated compound **2** (a11a-No60), the presence of an intermolecular 2.28-Å Cl2•••Cl2′ contact is much too short. No unreasonably short intermolecular contacts would exist if the crystal contained only the major (85%) Cl2 enantiomer in the asymmetric unit of the crystal (Figures S24 and S25) and all symmetry-related asymmetric units. However, for the asymmetric unit containing just the minor 15% enantiomer, atom Cl2′ is involved in a somewhat short intermolecular Cl2′•••H13′ contact of 2.68 Å. This is 0.32 Å shorter than the van der Waals value and might indicate that having this enantiomer in the asymmetric unit would be unreasonable unless this enantiomer and its symmetry-related ones slip and/or tilt slightly with respect to one another in a concerted manner when packing to give a second ordered domain. This shift/tilt seems to be consistent with the different C–C–Cl2 angles of 118.7° and 119.4° at carbon C13 as compared to the C–C18–Cl2′ angles of 109.6° and 129.5°, because the major 85% enantiomeric form present in the asymmetric unit (Figures S24 and S25) has normal metrics.

Once one of the minor 15% Cl2′ enantiomeric forms present in the asymmetric unit of Figure S25 packs in the asymmetric unit volume of its unit cell, other enantiomers with proper chirality could pack in a second ordered domain with Pbca symmetry that would avoid the short Cl2′•••Cl2 contacts that would be present if the 85% and 15% domains were not each ordered and separated. The apparent 85/15 disorder must be the result of their unit cells and asymmetric unit volumes being the virtually identical, similarly oriented, and translationally aligned. Both domains would be ordered and have their molecules related by the Pbca symmetry operations. Each superimposed asymmetric unit would appear to contain 85% of one enantiomer and 15% of the other enantiomer. This 85/15 ratio presumably reflects the relative enantiomeric packing preferences/desirabilities of **1** with hexafluorophospate anions and Pbca space group symmetry. The hexafluorophosphates would appear to be ordered and occupying essentially the same positions in both superimposed asymmetric units and unit cells.

Inspection of the data for **1** (q01i) did not reveal unindexed systematic reflections, and thus there is no evidence of a missed supercell. The electron density assigned as the minor 15% Cl2′ can therefore be ascribed to ordering effects as described here, rather than a supercell that would be associated with a modulation phenomenon.

Asymmetric Unit of the Major Domain for the Solid-state Structure of Compound 1.

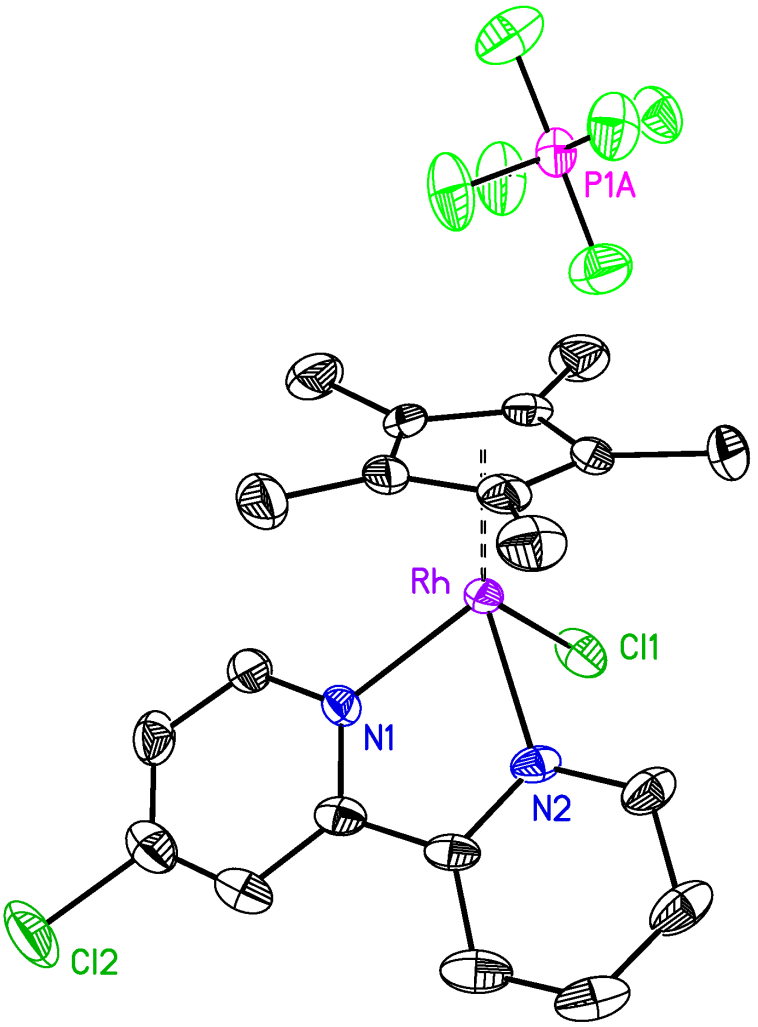

Figure S24. Solid-state asymmetric unit for **1** in the major 85% domain. An apparently fully-ordered nearby hexafluorophosphate counteranion is similarly positioned in both domains. Displacement ellipsoids are shown at the 50% probability level.

Asymmetric Unit of the Apparently Disordered Crystal Structure for Compound 1.

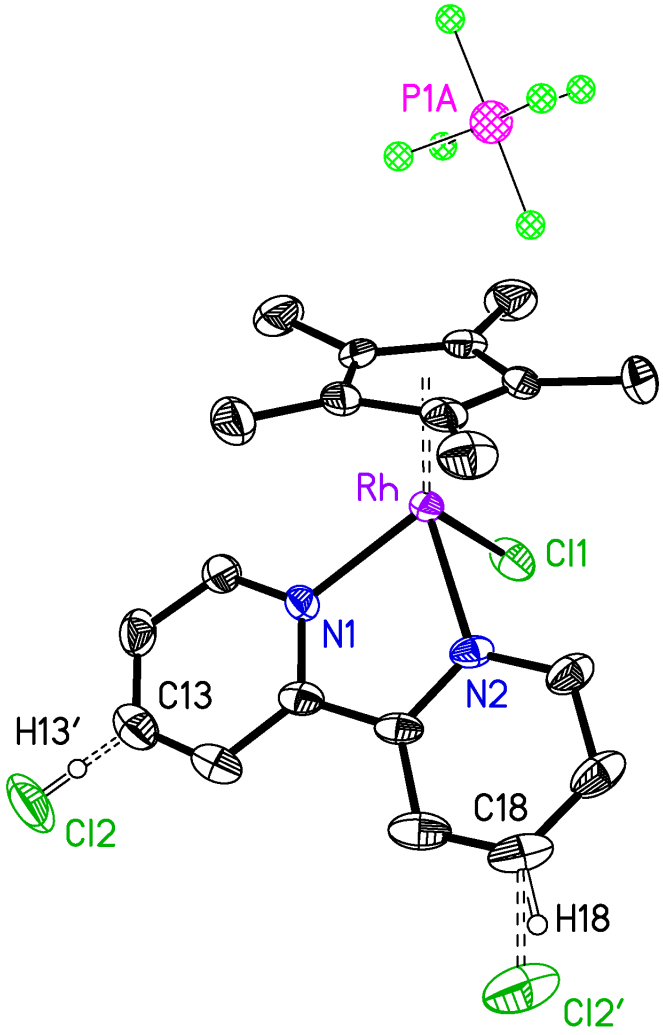

Figure S25. Asymmetric unit of the apparently disordered crystal structure for **1.** The asymmetric unit of the major 85% domain contains the Cl2 cationic species shown in Figure S24 while the asymmetric unit of the minor 15% domain contains its Cl2′ enantiomer. All atoms except Cl2, H18, Cl2′ and H13′ occupy essentially identical positions in the asymmetric units of both domains that utilize Pbca symmetry. This results in an apparent 85/15 disorder for the Cl substituent where the asymmetric unit 85% of the time contains Cl2 bonded to C13 and H18 bonded to C18 (bonds to atoms associated with the major domain are shown with hollow bonds). The asymmetric unit of the minor 15% domain has Cl2′ bonded to C18 and H13′ bonded to C13 (bonds to atoms associated with the minor domain are shown with dashed hollow bonds). Since any slight offsets of the enantiomeric Cl2′-substituted bipyridine ligands upon packing could not be detected, both enantiomers are shown and were modeled with a common bipyridine moiety as well as a common [Cp*RhCl] core (bonds between the apparently nondisordered atoms are shown with solid bonds). The hexafluorophosphate counteranion (drawn with cross hatched circles that are connected by solid lines) appears to be fully ordered and always present with the same orientation in both

domains. All H-atoms except H13′ and H18 are omitted for clarity. Displacement ellipsoids are shown at the 50% probability level.

Refining the Pbca model for **1** with Cl2′ and H13′ removed while still refining the occupancy factors for Cl2 and H18 as a free variable resulted in a higher R1 of 0.0554, an occupancy factor of 0.84 for Cl2 and H18 and a difference Fourier with the highest peak of 3.22 $e^{-}/Å^{3}$ at the Cl2′ site.

Special Refinement Details for 2

Initial structure solution and refinement of compound **2** in the centrosymmetric space group Pbcn (No. 60) refined to $R_1 = 0.0772$ and revealed 53/47 substitutional disorder involving the single nitro substituent. When checking intermolecular interactions, it was observed that the disordered nitro groups had intermolecular contacts for two symmetry-related O2A atoms that were much too short (O•••O, 1.421 Å). This could not be correct since the short contact involved two symmetry-related atoms of the minor 15% enantiomer present in the asymmetric unit of the Pbcn structure. A situation like that encountered for **1** (q01i) was an unlikely packing possibility in this case considering the rather large size of the nitro groups. It was suspected that (*i*) this nearly 50/50 disorder of the nitro groups might be the result of improperly-imposed crystallographic symmetry and that (*ii*) structure solution and refinement in another, lower-symmetry, space group might eliminate the aforementioned problematic intermolecular contacts.

Analysis of the systematic absences expected for **2** with space group Pbcn provided a clue about the proper space group. One of the glide planes (b-glide for Pbcn) had quite low <I> and <I/σ(I)> values but a significant (208/1082) number of I>3σ(I) systematic absence violations. So, this glide plane was changed to a 2_1 screw axis and the structure solution and refinement was carried out again in the noncentrosymmetric space group $Pna2_1$ (No. 33) with appropriately permuted lattice constants and two formula units per asymmetric unit. The new solution and refinement in noncentrosymmetric space group $Pna2_1$ had only a single nitro substituent on each bipyridyl ligand and avoided the aforementioned short contacts. This structure (a11a-No33) in $Pna2_1$ refined to $R_1 = 0.0482$ and was therefore taken as the preferred and correct description. (The anisotropic displacement parameters for atom C5A were mildly restrained.) As expected, CheckCIF/PLATON indicates a 91% pairwise fit of atoms from the two formula units in noncentrosymmetric structure a11a-No33 in space group $Pna2_1$ to corresponding atoms in a single formula unit in the centrosymmetric structure in space group Pbcn. This is completely in line with the analysis reported here. For clarity, the alternative refinement in Pbcn has been fully refined, provided to the Cambridge Structural Database (CSD) as structure a11a-No60, and accompanies this report for comparison to the preferred a11a-No33.

As with **2**, one of the glide planes in **1** (c-glide for Pbca) had quite low <I> and <I/σ (I)> values but a significant (221/1082) number of I>3σ(I) systematic absence violations. So, in order eliminate the possibility that the short 2.28-Å Cl2•••Cl2′ was not be due to imposed space group symmetry, this glide plane was changed to a 2_1 screw axis and the structure solution and refinement was redone in the noncentrosymmetric space group $Pca2_1$ with appropriately permuted lattice constants and two formula units per asymmetric unit. This refinement of **1** led to a slightly lower R_1 value but had extremely high correlations between parameters of the two formula units within the asymmetric unit. Unlike the two formula units in **2** in which only some pairs of atoms are related by inversion symmetry, all pairs of atoms in the noncentrosymmetric asymmetric unit of **1** appear to be 100% related by the crystallographic inversion center that was included in the original Pbca refinement. Considering this, we have chosen to present the centrosymmetric structure q01i in Pbca as the preferred and most correct structure solution and refinement for **1** in this report.

Considering the two mono-substituted bipyridyl derivatives explored in this work, we note that, in general, different crystallization behaviors are not unexpected when otherwise quite similar molecules (pairs of enantiomers in the present case) have one common part that differs considerably in size. Even though the nitro and chloro groups substitute the bipyridyl ligands in **1** and **2** at identical (4 and 4′) positions, the nitro group in **2** is considerably larger than the Cl in **1** and Cl is much closer in size to the bipyridyl hydrogen that is being replaced. Centrosymmetric structures for crystals of both **1** and **2** containing different compact polyatomic anions solve and refine reasonably well with disordered asymmetric units that have short intermolecular contacts between the apparently 85/15 disordered chloro or 53/47 disordered nitro substituents. Reducing the space group symmetry allowed the apparent 53/47 nitro-group disorder to be resolved/eliminated in **2** but this could not be done for the apparent 85/15 chloro-group disorder in **1**; this situation in the case of **1** is attributable to the more similar sizes of the two Cl-substituted enantiomers that are crystallizing/packing in what appear to be separate solid-state domains.

Regarding the identity of the counteranion in the structure of **2**, triflate was utilized in this case because efforts relying on PF_6^- were unsuccessful. Several attempts were made to grow diffraction-quality crystals of **2** with PF_6^- but ultimately a crystal could only be obtained when a special batch of the triflate salt of the rhodium cation was prepared for this purpose. All other characterization work for **2** was carried out with the PF_6^- salt, including the satisfactory elemental analysis. The standard PF_6^- was found to be suitable for all characterization, including diffraction analysis, in the case of **1**, so triflate was not explored in that case. However, we note that the difference in counteranion identity would almost certainly contribute to the differences in crystal packing behaviors described for **1** and **2**.

Solid-State Non-centrosymmetric Structure of the Molecular Cation in Compound 2

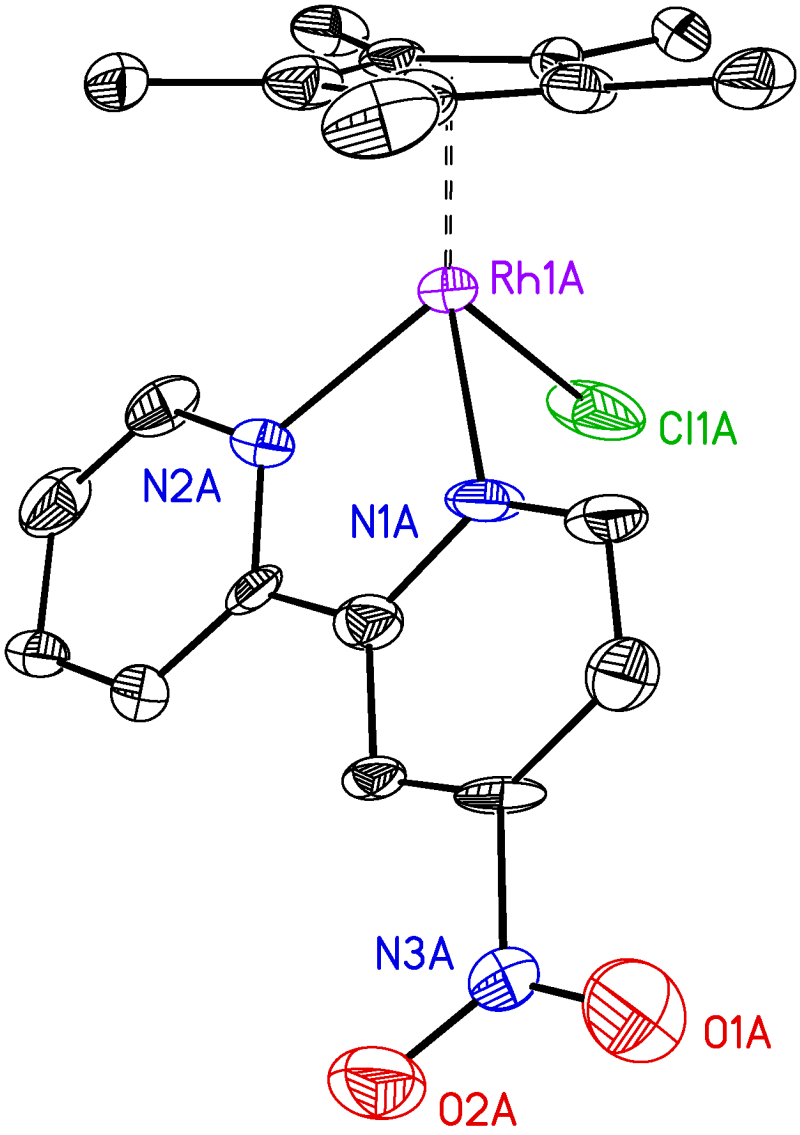

Figure S26. Solid-state structure for the first of two enantiomeric molecular cations present in the asymmetric unit of **2** in a11a-No33. The triflate counteranions, the second enantiomeric molecular cation, and all hydrogen atoms are omitted for clarity. Displacement ellipsoids are shown at the 50% probability level.

Full Asymmetric Unit of Compound 2 in (Correct) Non-centrosymmetric Space Group $Pna2_1$ (Structure: a11a-No33)

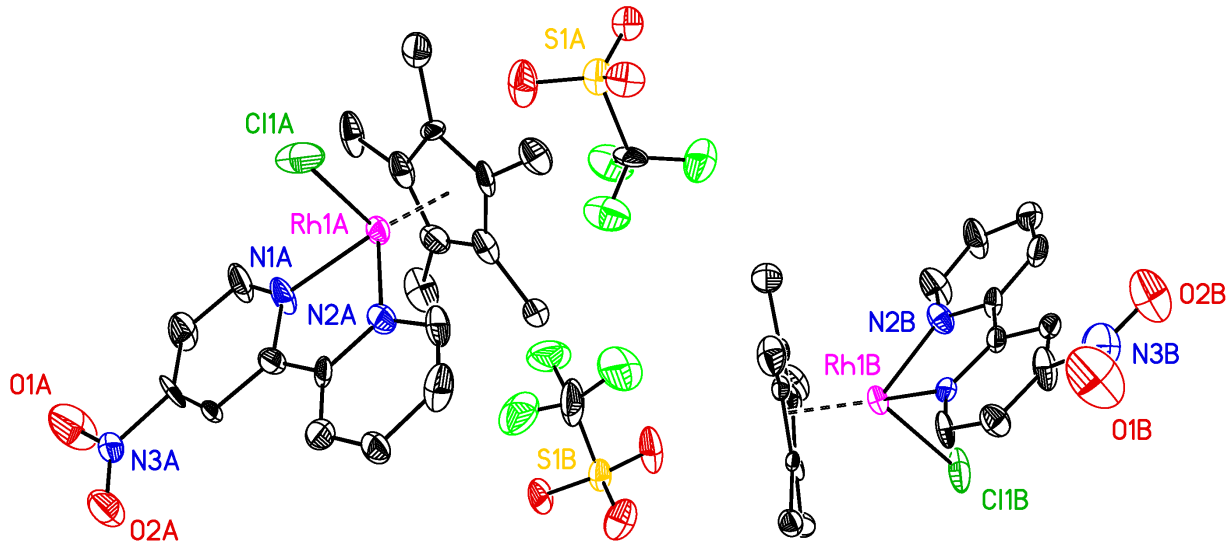

Figure S27. Solid-state structure of the asymmetric unit of compound **2** in the (correct) non-centrosymmetric space group $Pna2_1$ (Structure: a11a-No33) All H-atoms are omitted for clarity and displacement ellipsoids are shown at the 50% probability level.

Two Asymmetric Units of Compound 2 in (Incorrect Initial) Centrosymmetric Space Group Pbcn (Structure: a11a-No60)

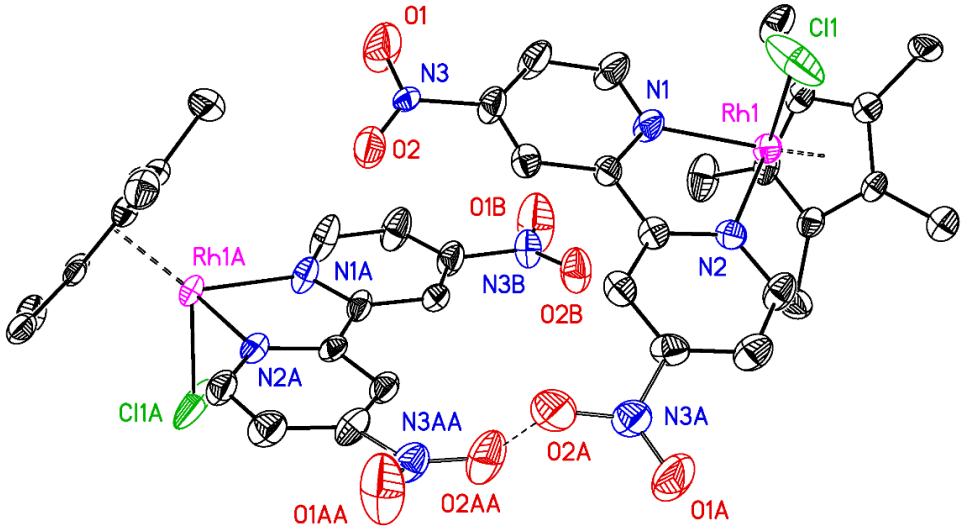

Figure S28. Solid-state structure of two asymmetric units of compound **2** in the (incorrect initial) centrosymmetric space group Pbcn (Structure: a11a-No60). The unacceptable short contact between nitrate groups is shown as the dashed line between atoms O2A and its symmetry-related O2AA. This contact of 1.421 Å is well below the 2.8 Å van der Waals value for two oxygen atoms. All H-atoms are omitted for clarity and displacement ellipsoids are shown at the 50% probability level.

Table S1 Crystal and refinement data for q01i.

	Compound 1 (q01i)
CCDC accession code	2203159
Empirical formula	$C_{20}H_{22}Cl_2F_6N_2PRh$
Formula weight	609.17
Temperature	200(2)
Wavelength	1.54184
Crystal system	orthorhombic
Space group	Pbca (No. 61)
a	13.1255(3)
b	12.7366(3)
c	27.4694(7)
α	90
β	90
γ	90
Volume	4592.18(19)
Z	8
Density (calculated)	1.762 g/cm^3
Absorption coefficient	9.374 mm^{-1}
F(000)	2432
Crystal size	0.085 × 0.067 × 0.060 mm^3
Theta range	3.22 to 70.32°
Index ranges	$-15 \le h \le 15$, $-15 \le k \le 15$, $-29 \le l \le 32$
Reflections collected	40635
Independent reflections	4291 [R_{int}=0.0533, R_{sigma}=0.0339]
Completeness/θ_{max}	99.7% / 66.00°
Absorption correction	Multi-scan
Max./Min. Transmission	0.753/0.511
Refinement method	Full-matrix least squares on F^2
Data/restraints/parameters	4291/0/305
Goodness-of-fit on F^2	1.076
Final R indices [I>2σ(I)]	R_1= 0.0478, wR_2= 0.1062
R indices (all data)[a,b]	R_1= 0.0490, wR_2= 0.1067
Largest diff. peak & hole	1.66/-1.00 e$^-$/Å^{-3}

[a] $R_1 = \Sigma||F_o|-|F_c|| / \Sigma|F_o|$ [b] $wR_2 = [\ \Sigma\ [w(F_o^2-F_c^2)^2] / \Sigma\ [w(F_o^2)^2]\ ]^{1/2}$

Table S2. Crystal and refinement data for a11a-No33 and a11a-No60.

	Compound 2 (a11a-No33)	**Compound 2 (a11a-No60)**
CCDC accession code	2370048	2203160
Empirical formula	$C_{21}H_{22}ClF_3N_3O_5SRh$	$C_{21}H_{22}ClF_3N_3O_5SRh$
Formula weight	623.83	623.83
Temperature	120(2)	120(2)
Wavelength	0.71073	0.71073
Crystal system	orthorhombic	orthorhombic
Space group	$Pna2_1$ (No. 33)	Pbcn (No. 60)
a	13.676(3)	15.898(3)
b	22.527(5)	22.527(5)
c	15.898(3)	13.676(3)
α	90	90
β	90	90
γ	90	90
Volume	4897.9(17)	4897.9(17)
Z	8	8
Density (calculated)	1.692 g/cm^3	1.692 g/cm^3
Absorption coefficient	0.952 mm^{-1}	0.952 mm^{-1}
F(000)	2512	2512
Crystal size	0.136 × 0.109 × 0.047 mm^3	0.136 × 0.109 × 0.047 mm^3
Theta range	1.57 to 26.42°	1.57 to 26.44°
Index ranges	$-17 \le h \le 17$, $-28 \le k \le 28$, $-19 \le l \le 19$	$-19 \le h \le 19$, $-28 \le k \le 28$, $-17 \le l \le 17$
Reflections collected	63592	62673
Independent reflections	10019 [R_{int}=0.0758, R_{sigma}=0.0355]	5040 [R_{int}= 0.0793, R_{sigma}= 0.0320]
Completeness/θ_{max}	99.9% / 25.242°	100.0% / 25.242°
Absorption correction	Multi-scan	Multi-scan
Max./Min. Transmission	0.745/0.694	0.745/0.694
Refinement method	Full-matrix least squares on F^2	Full-matrix least squares on F^2
Data/restraints/parameters	10019/7/642	5040/0/343
Goodness-of-fit on F^2	1.024	1.380
Final R indices [I>2σ(I)]	R_1= 0.0482, wR_2= 0.0956	R_1= 0.0772, wR_2= 0.1486
R indices (all data)[a,b]	R_1= 0.0759, wR_2= 0.1061	R_1= 0.0935, wR_2= 0.1543
Largest diff. peak & hole	1.11/-0.78 e$^-$/Å^{-3}	1.17/-1.20 e$^-$/Å^{-3}

[a] $R_1 = \Sigma||F_o|-|F_c|| / \Sigma|F_o|$ [b] $wR_2 = [\ \Sigma\ [w(F_o^2-F_c^2)^2] / \Sigma\ [w(F_o^2)^2]\ ]^{1/2}$